Real Time Indoor Positioning System for Smart Grid based on UWB and Artificial Intelligence Techniques

Long Cheng, *IEEE Senior Member*
Power System Consulting
ABB Inc.
Raleigh, NC, USA
dearlongcheng@gmail.com

Hao Chang, *IEEE Member*
Department of Electrical, Computer and Systems Engineering
Rensselaer Polytechnic Institute
Troy, NY, USA
samariumch@gmail.com

Kexin Wang
School of Mathematics
University of Minnesota, Twin Cities
Minneapolis, MN, USA
wang8051@umn.edu

Zhaoqi Wu
Department of Physics
University of Illinois at Urbana-Champaign
Champaign, IL, USA
zhaoqiw2@illinois.edu

***Abstract*— Indoor positioning system plays an important role in smart grid. Although GPS is the predominant outdoor positioning technology, it is unsuitable to be used in many fields of smart grid for three main reasons: first, signals sent from GPS could easily get blocked by solid materials such as metal or brick; second, the complex electromagnetic interference induced by electrical circuits greatly affects GPS signals; third, GPS can only achieve meter-level real time positioning accuracy, which is far from sufficient for many requirements of smart grid applications. Some other indoor positioning technologies, such as Bluetooth, Wi-Fi, ultrasound, infrared and RFID, fail in either the positioning accuracy, the positioning range, or the positioning speed required in many smart grid applications. Therefore, this paper proposes a real time indoor positioning system for smart gird based on a more promising technology, ultra-wideband (UWB). UWB is suitable for real-time localization in smart grid because UWB has short radio frequency pulse duration and wide bandwidth, which can minimize the effects of multipath interference and allow for high-resolution ranging and easier material penetration. In addition, since high-accuracy position information is required in many smart grid fields, a comprehensive framework integrating several artificial intelligence techniques, including outlier detection, line-of-sight/non-line-of-sight classification, filter design, range measurement correction and maximum likelihood localization estimation, is also proposed to further improve the positioning accuracy. At last, the performance of this system is verified through a series of experiments.**

Keywords—indoor localization, ultra-wideband, artificial intelligence, RTLS, smart grid

I. INTRODUCTION

Smart grid aims to make full use of digital information to improve reliability, security and efficiency of the electric power system and deploy real-time and automated technologies to optimize the physical operation of appliances concerning grid operations and status. The technology roadmap for the smart grid involves the deployment of the real-time indoor positioning system since accurate indoor localization information is very useful and necessary in many fields of smart grid. For example, more and more intelligent electronic devices such as smart meters are installed in smart gird for the purpose of sensing, controlling, or managing the status of smart grid [1-4]. The indoor positioning system can integrate the geospatial information to the data collected from intelligent electronic devices to provide more meaningful information to operators of smart gird [5]. For another example, the intelligent substation in smart grid also requires accurate positioning information to help monitor, measure, control and coordinate the operation of all equipment in the substation, improve the level of safe and stable operation of substation, reduce maintenance costs and ensure personnel safety. Especially, the personnel positioning requires accurate real-time indoor positioning system during the substation inspection and maintenance process since there are some dangerous equipment on the inspection route and the indoor positioning system can help monitor the real-time position of the maintenance staff and warn them to stay away from the dangerous equipment.

Traditional localization technology, GPS (Global Positioning System), is the predominant outdoor positioning technology. However, it is unsuitable, inaccurate and unreliable to be used in many smart grid applications, since it is limited by the penetration ability of GPS signals against solid objects such as walls or ceilings [6]. Meanwhile, the GPS signals are greatly affected by the complex electromagnetic interference induced by electrical circuits, resulting in large positioning errors. In addition, GPS can only achieve meter-level real time positioning accuracy, while many fields of smart grid require decimeter-level or even centimeter-level positioning accuracy. Hence, a positioning system with higher localization accuracy is desired. Several different positioning technologies such as RFID, Wi-Fi, ultrasound, Bluetooth, ZigBee and infrared have been explored for real-time indoor localization. Wi-Fi positioning uses a positioning method based on signal strength. Its positioning accuracy is about 5-10 m and can be easily affected by environmental interference. RFID technology has low positioning accuracy and weak communication capability. ZigBee is a short-range, low-power wireless network protocol that uses Received Signal Strength Indicator (RSSI) for positioning, resulting in a low data transmission rate and poor positioning accuracy [7]. All of these technologies could not achieve satisfactory performance in either the positioning accuracy, the positioning range, or the positioning speed required in many smart grid applications.

In recent decades, the ultra-wideband (UWB) has been introduced and shown better performance compared to other technologies in indoor localization [8]. UWB technology uses very narrow (nanosecond order) pulses of the time domain, which make the signal very wide in the frequency domain.

978-1-7281-3108-5/20/$31.00 ©2020 IEEE

UWB signals are defined as signals with either a large relative bandwidth that is typically larger than 20% of its center frequency, or a large absolute bandwidth that is greater than 500MHz. The short duration of UWB pulses assures the resistance against multipath interference and allows a supreme temporal and spatial resolution, enabling UWB positioning system to have centimeter-level positioning accuracy [9]. The high positioning accuracy is particularly important for many smart grid applications. Furthermore, compared with traditional narrowband radio frequency (RF) signals, UWB signals are more likely to pass through obstacles between the anchor and the tag with less delay and attenuation because of the low frequency of UWB pulses [10]. Meanwhile, the United States Federal Communications Commission (FCC) allocates a band of 3.1 GHz to 10.6 GHz for UWB to use, which has no interference to most of the Smart Grid wireless equipment and thus will not interrupt the normal operation of smart gird. In addition, the output power of UWB radio pulse signal is very low and even lower than the external noise, making the UWB signal has less negative effect on human and electronic equipment in smart grid. Therefore, UWB based indoor positioning system should be one of the most suitable choices for smart gird.

There are mainly three kinds of positioning algorithms used for UWB indoor positioning system: (1) angle of arrival (AOA); (2) time of arrival (TOA); and (3) time difference of arrival (TDOA). AOA requires large dimensions of antenna arrays and sensors, is subject to measure error accumulation [11], and is easily affected by many factors, such as antenna array geometry [12]. It is more complex compared to TOA and TDOA. TOA requires clock synchronization in all transmitters. So any delay or error in clock synchronization could have large negative impact on the positioning accuracy. TDOA is a better choice if no synchronization exists between the tag and the anchors when the anchors are synchronized among themselves [13]. If there is no common clock between nodes, distance between two nodes can be estimated by measuring the round-trip time between two transceiver nodes [14]. However, no matter which positioning algorithm is used, there are many factors that could affect the ranging accuracy, especially considering a realistic environment. The main sources of ranging error include non-line-of-sight (NLOS), multipath propagation, multiple access interface, and high time resolution of UWB signals [15].

Motivated by the advantages of UWB for indoor positioning system, in this paper, we designed a UWB based real-time indoor positioning system for smart gird and further improved its positioning accuracy by using several artificial intelligence and signal processing techniques.

II. Related Work

Researchers have explored different artificial intelligence and signal processing techniques to improve the positioning accuracy of the UWB based indoor positioning system. A method combining the maximum likelihood principle with range error methods and fingerprints for UWB localization was proposed to mitigate the ranging errors caused by the direct path is blocked by obstacles [16]. The authors in [17] designed a UWB indoor positioning system using an adaptive leading-edge detection algorithm to differentiate LOS and NLOS to improve the ranging accuracy. The authors in [18] developed an extended H∞ filter based algorithm to estimate the target's real-time location and velocity using UWB signals. A 3D Chan algorithm and a modified propagator method were proposed in [19] for position determination and time delay estimation in a UWB positioning system. The researchers in [20] presented a space-time Bayesian compressed sensing algorithm for a UWB indoor positioning system to improve the system's tolerance to noise while reducing the sampling rate. The authors in [21] studied the generalized Gaussian mixture filter, which approximates the likelihood associated with UWB range measurements, and compared it with extended Kalman filter. A sparse sensing framework for joint estimation of TOA and AOA in IR-UWB systems was proposed in [22]. A heuristics based method combining multi-cell method and Chan's method [23] was used in [24] to improve the UWB positioning accuracy, especially at boundaries.

III. Real-time Indoor Positioning System

This section introduces the architecture design of the proposed UWB based real-time indoor positioning system, as well as the algorithms that are used in this system to improve the positioning accuracy.

A. System Design

The anchor and tag modules of the designed positing system use the Decawave's DW1000 chip implemented with IEEE 802.15.4-2011 UWB compliant. ARM Cortex-M4 processor architecture based STM32F4 is used as the microcontroller for the anchor and tag module. In addition, the electronic switch, the serial port, the power interface, the omnidirectional antenna, the regulators, the crystals, the heat sink and some other necessary electronic components are integrated in the anchor and tag modules, as shown in Fig. 1.

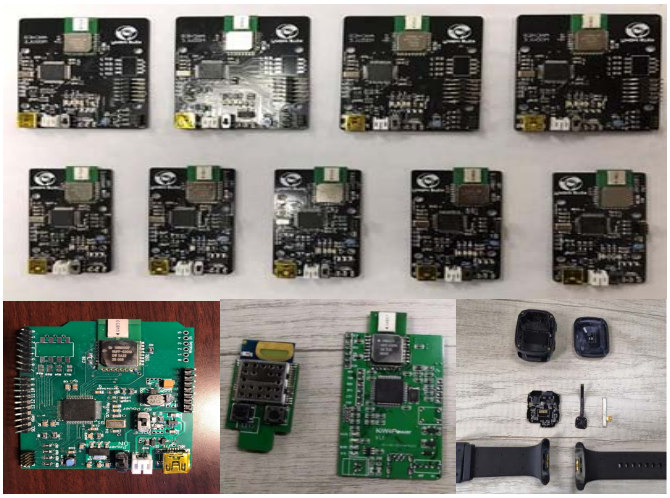

Figure 1. The hardware design of tags and anchors in our real-time indoor positioning system

The tag module is put on the object to be tracked and can be embedded into protective helmet, shoe, watch bracelet, or badge when tracking human position.

Four UWB anchors are usually required in the positioning system since at least three anchors are used as the reference nodes to determine the location of the tags, and one extra UWB anchor is used as the master anchor, which is connected to an upper computer through a Serial-to-USB converter to allow communication with the upper computer and is also responsible to communicate with the rest UWB tags and anchors in the indoor positioning system. For example, the upper computer can send commends to the master anchor to schedule the sleep/wake time for the rest anchors and tags, and set system parameters such as the update rate, the maximum numbers of tags and anchors in the system, and 3D/2D localization mode selection. Meanwhile, the master anchor can also transfer the range measurements and tag position information to the upper computer. And then the upper computer can store the information in both the local database and the database hosted on the server, as well as showing the real-time positions of tags on the screen, as shown in Fig. 2. The server can further send the position information to mobile phones.

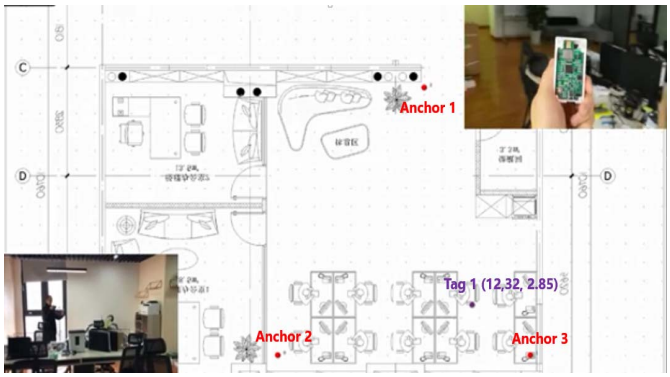

Figure 2. Postions of anchors and tags are shown on the screen of the upper computer

The system uses two-way time of flight (TW-TOF) method for the range measurement and uses trilateration method for position calculation. In 2D localization, at least three ranges from a tag to three different anchors are needed to determine the position of the tag. In 3D localization, at least four ranges from a tag to four different anchors deployed at different heights are required. Some methods can be used to reduce the number of ranges required to locate an object in 2D or 3D localization, which we will not discuss here. If extra anchors are put in the system and more than the minimum number of range measurements are given, probably there is no unique position can be determined using the trilateration algorithm since the range measurements usually contain error and noise. Selecting different reference nodes in the trilateration algorithm can result in different positions. To account for this scenario, the non-linear least squares solver [25] is added in the system in order to obtain the optimal location solution.

B. Outlier Detection

Due to inevitable hardware constraints and external environment effects such as shadowing, the range measurements are sometimes contaminated with outliers, resulting in misleading position estimation. Simply applying some existing outlier detection methods on the range measurements is not a good solution since the existing outlier detection methods have their drawbacks and might not be suitable for a real-time indoor locating system.

Therefore, in our indoor positioning system, we propose a real-time outlier detection approach with the ability to take the movement speed of the tag and the update frequency of the system into consideration, instead of simply deleting the outliers using pure statistical analysis. This filter is named as Cheng filter.

We use a sliding window to select the most recent n range measurements to form a data set, $M = \{m_1, m_2, ..., m_n\}$, use $median(M)$ to denote the median of this data set. And then we define the median absolute deviation (MAD) estimator as

$$MAD = 1.4826 \times median(|\, m_i - median(M)\,|) \qquad (1)$$

where the coefficient 1.4826 is selected to make sure the expected value of MAD equals the standard deviation for normal distribution measurements.

Meanwhile, to avoid a situation where more than half of the data in the dataset have the same value, the MAD will be zero, resulting in any data not equal to that value is identified as an outlier. We will relax the MAD cutoff condition by considering the movement speed of the tag and the update frequency of the system. Suppose the update frequency of the indoor locating system is f Hz and the maximum movement speed of the tag is v cm/s, which can be determined in advance based on the real situation. So the maximum distance that the tag can move between two range measurements is v/f cm, which also means the largest difference between two successive range measurement values allowed in the system can be v/f cm. Considering measurement noise, we multiple the largest difference with a coefficient 1.2. So we relax the MAD cutoff condition by preventing any successive data that within a $1.2v/f$ cm difference being classified as outliers.

C. LOS/NLOS Classification

Even though the TW-TOF can reduce the range measurement error caused by improper time synchronization, the range measurement is still affected by relative clock drift or clock deviation. In addition, NLOS could also affect the range measurement. In our system, the LOS range measurement variance σ^2_{LOS} is used to roughly distinguish LOS range measurement from NLOS range measurement. Whenever a range is measured with a pair of UWB tag and anchor, if this range measurement variance is larger than σ^2_{LOS}, this range measurement is classified as a NLOS range measurement. Otherwise, it is a LOS range measurement.

D. Filter Design

Since Kalman filter has been known as an excellent filter for data prediction and object tracking, a two-layer Kalman filter is designed in our indoor positioning system. The first layer is to use a Kalman filter to filter each original range measurement and the second layer is to use Kalman filter again

to filter the calculated position coordinates. In this way, both the range measurements and the final position data will be more accurate and stable.

The state equation of the system is shown as follows.

$$X_{k+1} = \phi X_k + W_k \tag{2}$$

where X_k denotes a state vector with dimension n at time k, Φ denotes a nxn state transition matrix of the process from the state at time k to the state at time k+1, and W_k denotes a noise vector with dimension p at time k.

The measurement equation of the system is shown as follows.

$$Z_k = HX_k + V_k \tag{3}$$

where Z_k denotes a measurement vector with dimension *m* at time *k*, H denotes a mxn matrix connecting the state vector and the measurement vector, and V_k denotes a measurement error vector with dimension m.

Set W_k and V_k as Gaussian noise. The summary of the Kalman Filter algorithm is as follows.

1. Calculate Kalman Gain:

$$K_k = P_k' H^T (HP_k' H^T + R)^{-1} \tag{4}$$

2. Update Estimate:

$$\hat{x}_k = \hat{x}_k' + K_k(z_k - H\hat{x}_k') \tag{5}$$

3. Update Covariance:

$$P_k = (I - K_k H)P_k' \tag{6}$$

4. Project into k+1:

$$\hat{x}_{k+1}' = \phi \hat{x}_k \tag{7}$$

$$P_{k+1} = \phi P_k \phi^T + Q \tag{8}$$

where

$$Q = E[W_k W_k^T] \tag{9}$$

$$R = E[V_k V_k^T] \tag{10}$$

This two-layer Kalman filter has a good performance in predicting the measurements and the states of the system, as well as reducing the NLOS error, improving the positioning accuracy of the system.

E. Range Measurement Correction with Regression Analysis

Though the circuits of our UWB anchor and tag are well designed and delicate calibrations are carefully done for antenna delay and crystal tuning, the range measurement is still not accurate. In order to correct the range measurement, a regression analysis is applied to estimate the relationship between the range measurement and the actual distance between the anchor and the tag.

After the regression model is trained, this regression model is integrated in the range measurement function to transfer the original range measurement to a more precise range output.

F. Maximum Likelihood Localization Estimation

In order to further improve the positioning accuracy, we are motivated to take advantages of some prior information that will be available in a real indoor environment, including knowledge of the indoor environment layout (such as the geometry of the indoor environment and the positions of other objects that might affect LOS between tag and anchor), knowledge of the range measurement error (such as the probability density functions of range measurement errors when tags are in different positions and the prior probabilities of LOS/NLOS happens) and knowledge of the position fingerprints that set up in advance.

First, we need to build an Undetected Direct Path (UDP)/Detected Direct Path (DDP) database according to the actual indoor environment based on the method proposed in [16]. Second, use $z = (x, y)^T$ to indicate the position of a tag and use $z_n = (x_n, y_n)^T \quad (n = 1, 2, ..., N)$ to indicate the position of the *n*th anchor.

If the anchor and the tag are in DDP range, the range measurement can be formed as

$$r_n = d_n + \varepsilon_{n,DDP} \tag{11}$$

where d_n is the LOS distance between the anchor and the tag

$$d_n = \sqrt{(x - x_n)^2 + (y - y_n)^2} \tag{12}$$

$\varepsilon_{n,DDP}$ is the range error and suggested to be represented as the following equation based on the study in [26].

$$\varepsilon_{n,DDP} = \gamma \log(1 + d_n) \tag{13}$$

where γ is a random variable in Gaussian distribution with mean m_γ and standard deviation σ_γ. The value of m_γ, σ_γ can be determined by real experiments with the UWB indoor positioning system. Based on Eq. 11 and Eq. 13, γ can represented as

$$\gamma = \frac{r_n - d_n}{\log(1 + d_n)} \tag{14}$$

Based on Eq. 13, $\varepsilon_{n,DDP}$ is Gaussian distribution with mean

$$m_{n,DDP} = m_\gamma \log(1 + d_n) \tag{15}$$

and standard deviation

$$\sigma_{n,DDP} = \sigma_\gamma \log(1 + d_n) \tag{16}$$

So the probability density function of r_n can be represented as

$$PDF_{DDP}(r_n) = \frac{1}{\sqrt{2\pi}\sigma_{n,DDP}} \exp\left[-\frac{(r_n - d_n - m_{n,DDP})^2}{2\sigma_{n,DDP}^2} \right] \tag{17}$$

If the anchor and the tag are in UDP range, the range measurement can be formed as

$$r_n = d_n' + \varepsilon_{n,UDP} \tag{18}$$

where d_n' ($d_n' > d_n$) is the shorted path between the anchor and the tag, which can be computed using a ray tracing algorithm.

$\varepsilon_{n,UDP}$ is represented as

$$\varepsilon_{n,UDP} = \gamma \log(1 + d_n') \tag{19}$$

where γ is a random variable in Gaussian distribution with mean m_γ and standard deviation σ_γ . Like Eq. 13, $\varepsilon_{n,UDP}$ is Gaussian distribution with mean

$$m_{n,UDP} = m_\gamma \log(1 + d_n') \tag{20}$$

and standard deviation

$$\sigma_{n,UDP} = \sigma_\gamma \log(1 + d_n') \tag{21}$$

Under the UDP condition, we can rewrite Eq. 18 as

$$r_n = d_n + \tilde{\varepsilon}_{n,UDP} \tag{22}$$

So the probability density function of r_n can be represented as

$$PDF_{UDP}(r_n) = \frac{1}{\sqrt{2\pi}\tilde{\sigma}_{n,UDP}} \exp\left[-\frac{(r_n - d_n - \tilde{m}_{n,UDP})^2}{2\tilde{\sigma}_{n,UDP}^2} \right] \tag{23}$$

The position of a tag can be classified into two categories, one is DDP, denoted by $C_{DDP}(z)$, and another one is UDP, denoted by $C_{UDP}(z)$. So the probability density function of r can be represented as

$$PDF(r) = \prod_{n \in C_{DDP}(z)} PDF_{DDP}(r_n) \times \prod_{n \in C_{UDP}(z)} PDF_{UDP}(r_n) \tag{24}$$

Therefore, the likelihood function can be calculated as

$$\begin{aligned} \ell(r) = &- \sum_{n \in C_{DDP(z)}} \ln \sigma_{n,DDP} - \sum_{n \in C_{DDP(z)}} \frac{(r_n - d_n - m_{n,DDP})^2}{2\sigma_{n,DDP}^2} \\ &- \sum_{n \in C_{UDP(z)}} \frac{(r_n - d_n - \tilde{m}_{n,UDP})^2}{2\tilde{\sigma}_{n,UDP}^2} - \sum_{n \in C_{UDP(z)}} \ln \tilde{\sigma}_{n,UDP} \end{aligned} \tag{25}$$

The maximum likelihood localization estimation searches for the maximum $\ell(r)$ over all feasible tag position $z = (x, y)^T$.

IV. Experiment Results

A. Outlier Detection and Measurement Filtering (ODMF)

In order to verify the effectiveness of our proposed ODMF design, two experiments are conducted. In the first experiment, the tag is placed at 11 different locations. The actual distance from the tag to the anchor is 20cm, 50cm, 100cm, 200cm, 300cm, 400cm, 500cm, 600cm, 700cm, 800cm, and 900cm respectively. At each location, 800 time-series range measurements are taken. The original range measurements are shown in Fig.3. It can be seen that there are many outliers and noises in the range measurements, which will result in much larger errors in the final position calculation.

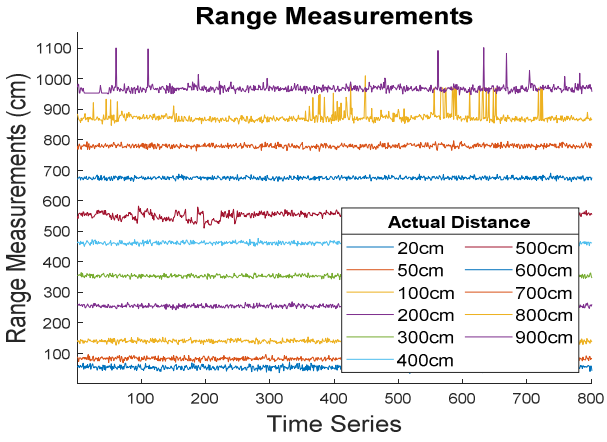

Figure 3. Original range measurements taken at 11 different positions

In the second experiment, our proposed outlier detection algorithm and the Kalman filter algorithm are integrated into our UWB indoor positioning system. Repeat the steps in the first experiment and now the range measurements are shown in Fig. 4. Now the measurements become very smooth and stable, with no outlier, which will greatly increase the position accuracy.

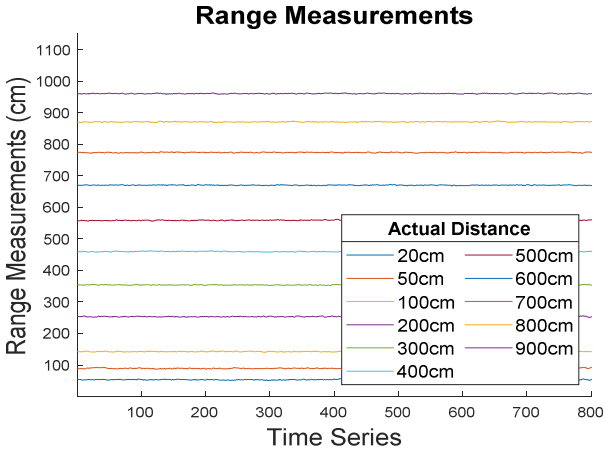

Figure 4. Range measurements taken at 11 different positions after applying outlier detection algorithm and Kalman filter

B. Range Measurement Correction (RMC)

Even though the range measurements are now stable, there are many systematic errors in the measurement. For example, in Fig. 5, when the actual distance between the tag and the anchor is 50cm, the range measurement is close to 100cm; when the actual distance is 600cm, the measurement is about 680 cm. The relationship between the actual distance and the range measurement is summarized in Fig. 5.

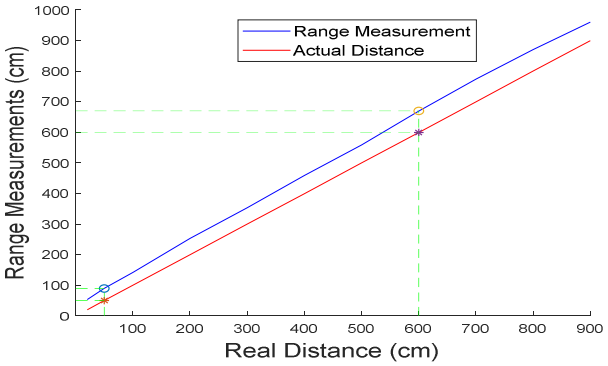

Figure 5. The relationship between the actual distance and the range measurement

It can be seen from Fig. 5 that the relationship between the actual distance and the range measurement is not linear. So we conduct a non-linear regression analysis and apply the RMC in our UWB indoor positioning system. In our system, we use a polynomial of degree 3, shown in Eq. 26, to correct the range measurements.

$$y = 0.001x^2 + 0.9028x - 29.7469 \tag{26}$$

Repeat the steps in the first experiment and now the range measurements are shown in Fig. 6. Now it can be seen that the range measurements are highly accurate.

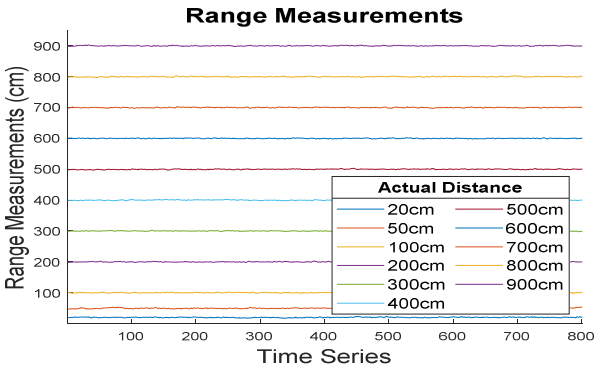

Figure 6. Range measurements taken at 11 different positions after applying range measurement correction

C. *LOS/NLOS Classification and Maximum Likelihood Localization Estimation (LCMLLE)*

Even though the range measurements are now both stable and accurate after applying ODMF and RMC, the range measurement can still be affected if there are obstacles that block the LOS. Therefore, LCMLLE is integrated in our UWB indoor locating system to reduce the effect of NLOS on range measurements.

Fig. 7 shows the installation of anchors in a 110 kV substation. Fig. 8 shows a floor plan (5256cm*3088cm) with an obstacle and indicates the LOS zone and NLOS zone separated by the obstacle for Anchor 1. We randomly select 30 positions in this area, get 100 position measurements for each position, and finally calculate the root mean square error (RMSE) to evaluate the positioning accuracy of our UWB indoor positioning system when integrating different techniques, i.e. ODMF, RMC and LCMLLE. The RMSE is defined as

$$RMSE = \sqrt{\sum_{i=1}^{n} \frac{(\hat{x}_i - x_i)^2 + (\hat{y}_i - y_i)^2}{n}} \tag{27}$$

where $(\hat{x}_i, \hat{y}_i)$ is the measured position of the tag and (x_i, y_i) is the actual position of the tag.

Figure 7. The installation of anchors in a 110 kV substation

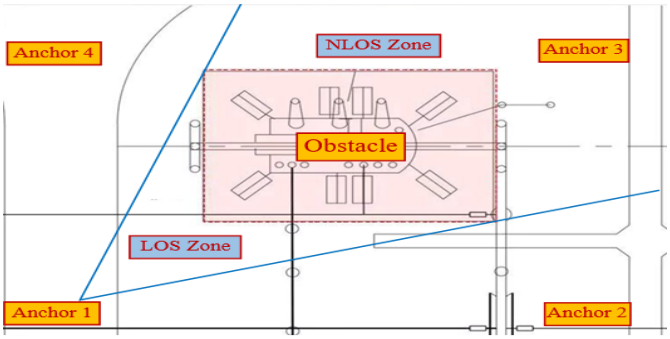

Figure 8. The floor plan and the LOS/NLOS zones for an anchor

Fig. 9 shows the positioning accuracy when integrating different proposed techniques into the UWB indoor positioning system. After applying ODMF, RMC and LCMLLE together, the average positioning error is reduced from 221cm to 14cm, which demonstrates the effectiveness of our proposed methods in improving the positioning accuracy.

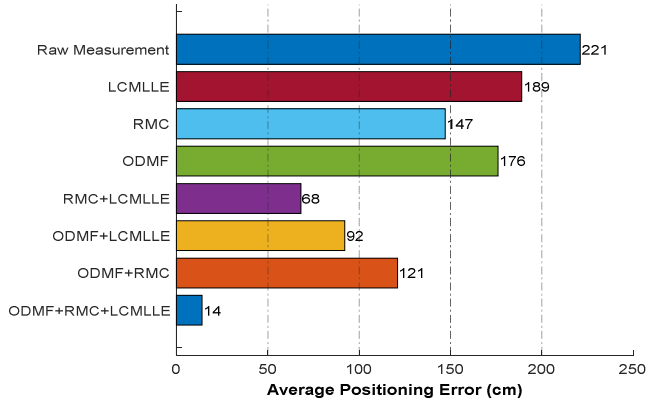

Figure 9. Impact of different techniques on positioning accuracy

V. CONCLUSION

This paper proposes a real-time indoor positioning system for smart gird based on UWB. To further improve the positioning accuracy of the indoor positioning system, a comprehensive framework based on artificial intelligence and signal processing techniques is also proposed. The techniques in the framework include outlier detection based on MAD and system parameters, LOS/NLOS classification based on range measurement variance, two-layer Kalman filter design, measurement correction based on regression analysis, and maximum likelihood localization estimation based on prior knowledge about the real indoor environment. Experiment results show that this framework is both robust and effective in increasing the positioning accuracy of the indoor positioning system.

In the near future, we will explore the random projection methods [27, 28] to reduce the number of range measurements needed to locate the position of the tag for an indoor locating system with a high update frequency. In addition, we will also investigate the compressed sensing methods to recognize human activities [29-33] using the UWB measurements from the indoor positioning system, making the UWB indoor positioning system more useful for the smart gird.

REFERENCES

[1] L. Cheng, C. You, and L. Chen, "Identification of power line outages based on PMU measurements and sparse overcomplete representation," *IEEE 17th International Conference on Information Reuse and Integration*, pp. 343-349, 2016.

[2] L. Cheng, L. Wang, and F. Gao, "Power system fault classification method based on sparse representation and random dimensionality reduction projection," in *Proc. 2015 IEEE Power & Energy Society General Meeting*, pp. 1-5, 2015.

[3] L. Cheng, Z. Wu, R. Duan, et al, "Adaptive compressive sensing and machine learning for power system fault classification," *in Proceedings of 2020 IEEE SoutheastCon*, March, 2020.

[4] L. Cheng, Z. Wu, S. Xuanyuan, et al, "Power quality disturbance classification based on adaptive compressed sensing and machine learning," *in 2020 IEEE Green Technologies Conference*, Oklahoma City, OK, 2020.

[5] T. A. Khan, A. B. Khan, M. Babar, et al, "Smart meter incorporating UWB technology," in *Proc. 2014 IEEE NW Russia Young Researchers in Electrical and Electronic Engineering Conference*, pp.75-78, 2014.

[6] J. Hightower, G. Borriello, "Location systems for ubiquitous computing," Computer, vol. 34, pp. 57-66, August 2001.

[7] Z. Song, G. Jiang, C. Huang, "*A survey on indoor positioning technologies*," in *Theoretical and Mathematical Foundations of Computer Science, Springer*, pp. 198-206, 2011.

[8] A. Alarifi, A. AI-Salman, M. Alsaleh, et al, "Ultra wideband indoor positioning technologies: analysis and recent advances," *Sensors (Basel)*, vol. 16, no. 5, pp. 1-36, May 2016.

[9] L. Zwirello, T. Schipper, M. Harter, et al, "UWB localization system for indoor applications: Concept, realization and analysis," *Journal of Electrical and Computer Engineering*, pp. 4-15, Jan 2012.

[10] J. Y. Lee, and S. Choi, "Through-material propagation characteristic and time resolution of uwb signal," *International Workshop on Ultra Wideband Systems Joint with Conference on Ultra wideband Systems and Technologies*, pp. 71-75, 2004.

[11] P. Kulakowski, J. Vales-Alonso, E. Egea-Lopez, et al, "Angle-of-arrival localization based on antenna arrays for wireless sensor networks," *Computer & Electrical Engineering*, vol. 36, no. 6, pp. 1181-1186, 2010.

[12] S. AI-Jazzar, A. Muchkaev, A. AI-Nimrat, et al, "Low complexity and high accuracy angle of arrival estimation using eigenvalue decomposition with extension to 2D AOA and power estimation," *EURASIP Journal on Wireless Communication and Networking*, pp. 1-13, 2011.

[13] J. Caffery, Jr., "Wireless location in CDMA cellular radio systems," *Boston, MA: Kluwer*, 2000.

[14] JY. Lee, R.A. Scholtz, "Ranging in a dense multipath environment using a UWB radio link," *IEEE Trans. Select. Areas Commun*., vol. 20, no. 9, pp. 1677-1683, Dec, 2002.

[15] S. Gezici, Z. Tian, G. B. Giannakis, et al, "Localization via ultra-wideband radios: A look at positioning aspects for future sensor networks," *IEEE Signal Processing Magazine*, vol. 22, pp. 70-84, 2005.

[16] E. Arias-de-Reyna, and U. Mengali, "A maximum likelihood UWB localization algorithm exploiting knowledge of the service area layout," *Wireless Personal Communications*, vol. 69, no. 4, pp. 1413–1426, May, 2012.

[17] M. Mahfouz, M. Kuhn, Y. Wang, et al, "Towards sub-millimeter accuracy in UWB positioning for indoor medical environments," *In Proceedings of the 2011 IEEE Topical Conference on Biomedical Wireless Technologies, Networks, and Sensing Systems*, pp. 83–86, Jan, 2011.

[18] F. Cao, M. Li, "An algorithm for UWB signals tracking based on extended H Filter," *Physics Procedia*, vol. 33, pp. 905–911, 2012.

[19] H. Jiang, Y. Zhang, H. Cui, et al, "Fast three-dimensional node localization in UWB wireless sensor network using propagator method digest of technical papers," In Proceedings of the 2013 IEEE International Conference on Consumer Electronics, pp. 627–628, Jan, 2013.

[20] D. Yang, H. Li, Z. Zhang, et al, "Compressive sensing based sub-mm accuracy UWB positioning systems: A space–time approach," *Digital Signal Processing*, vol. 23, no. 1, pp. 340–354, 2012.

[21] P. Muller, H. Wymeersch, and R. Piche, "UWB positioning with generalized Gaussian mixture filters," *IEEE Transactions on Mobile Computing*, vol. 13, no. 10, pp. 2406–2414, Oct, 2014.

[22] F. Wang, X. Zhang, "Joint estimation of TOA and DOA in IR-UWB system using sparse representation framework," *ETRI Journal*, vol. 36, no. 3, pp. 460–468, 2014.

[23] Y. Chan, and K.C. Ho, "A simple and efficient estimator for hyperbolic location," *IEEE Transactions on. Signal Processing*, vol. 42, no.8, pp. 1905-1915, Aug, 1994.

[24] S. Krishnan, P. Sharma, Z. Guoping, et al, "A UWB based localization system for indoor robot navigation," *In Proceedings of the IEEE International Conference on Ultra-Wideband*, pp. 77–82, 2007.

[25] S. Wright, and J. Nocedal, "Numerical optimization," *Springer Science*, vol. 35, pp. 67-68, 1999.

[26] B. Alavi, and K. Pahlavan, "Modeling of the TOA-based distance measurements error using UWB indoor radio measurements," *IEEE Communications Letters*, vol.10, no.4, pp. 275-277, 2006.

[27] L. Cheng, and C. You, "Hybrid non-linear dimensionality reduction method framework based on random projections," *IEEE International Conference on Cloud Computing and Big Data Analysis*, pp. 43-48, 2016.

[28] L. Cheng, C. You, and Y. Guan, "Random projections for non-linear dimensionality reduction," *International Journal of Machine Learning and Computing*, vol. 6, no. 4, pp. 220-225, 2016.

[29] L. Cheng, Y. Yu, X. Liu, et al, "Recognition of human activities using fast and adaptive sparse representation based on wearable sensors," *Proceedings of the 16th IEEE International Conference on Machine Learning and Applications (ICMLA)*, pp.944-949, 2017.

[30] L. Cheng, Y. Li, and Y. Guan, "Human activity recognition based on compressed sensing," *The 7th IEEE Annual Computing and Communication Workshop and Conference*, pp. 484-490, 2017.

[31] L. Cheng, Y. Guan, K. Zhu, et al., "Accelerated sparse representation for human activity recognition," *IEEE 18th International Conference on Information Reuse and Integration*, 2017.

[32] L. Cheng, C. You, Y. Guan, et al, "Body activity recognition using wearable sensors," *Computing Conference*, pp. 756-765, 2017.

[33] L. Cheng, Y. Guan, K. Zhu, and Y. Li, "Recognition of human activities using machine learning methods with wearable sensors," *The 7th IEEE Annual Computing and Communication Workshop and Conference*, pp. 86-92, 2017.